Discover Oncology

Analysis

Unveiling novel susceptibility genes and drug targets for basal cell carcinoma by a cross-tissue transcriptome-wide association study

Hong Sun[1] · Ling Li[1] · Xiu Xin[1] · Jingchao Yan[1] · Taomin Huang[1]

Received: 30 September 2024 / Accepted: 3 March 2025
Published online: 10 March 2025

Abstract

Objective To identify novel susceptibility genes and drug targets for basal cell carcinoma (BCC).

Methods We performed a transcriptome-wide association study (TWAS) to identified the susceptibility genes and potential drug targets for BCC. The cross-tissue TWAS was conducted to discover the candidate genes for BCC. Functional Summary-based Imputation (FUSION) analysis was used to validate these genes in the single tissues. Multimarker Analysis of Genomic Annotation (MAGMA) was employed to further screen candidate genes. Summary data-based Mendelian randomization (SMR) and colocalization analyses were applied to infer causal relationships between candidate genes and BCC. The expression pattern of the identified genes in single-cell types was also investigated. Function, pathway enrichment and disease connection analyses were performed to understand the biological implication of identified genes. Additionally, druggability of the identified genes was evaluated to discover potential candidate drugs for BCC.

Results Ninety-five genes were identified by cross-tissue TWAS analysis. Among them, 24 genes were confirmed by FUSION and MAGMA methods. Ten genes were further confirmed by SMR and colocalization analyses. Three genes were replicated by using another GWAS data. The potential interacting gene networks constructed with these identified genes were mainly involved in viral life cycle-HIV-1, GABAergic synapse, nicotine addiction, ether lipid metabolism, and mineral absorption pathways. AN-9 and amooranin might be candidate drugs for BCC.

Conclusions We have identified 10 susceptibility genes associated with BCC risk, which might deepen our comprehension of BCC pathogenesis and illuminating new avenues for therapeutic and preventive drug development.

Keywords Basal cell carcinoma · Cross-tissue TWAS · Susceptibility genes · Drug targets

Abbreviations

BCC	Basal cell carcinoma
TWAS	Transcriptome-wide association study
FUSION	Functional summary-based imputation
MAGMA	Multimarker analysis of genomic annotation
SMR	Summary data-based Mendelian randomization
UTMOST	Unified test for molecular signatures
FDR	False discovery rate

Supplementary Information The online version contains supplementary material available at https://doi.org/10.1007/s12672-025-02019-y.

✉ Jingchao Yan, jingchao.yan@fdeent.org; ✉ Taomin Huang, taominhuang@126.com | [1]Department of Pharmacy, Eye & ENT Hospital, Fudan University, Shanghai, China.

COJO Conditional and joint
cis-eQTL Cis-expression quantitative trait loci
HEIDI Heterogeneity in the dependent instrument
PP.H4 Posterior probability of H4

1 Introduction

Basal cell carcinoma (BCC) is one of the most prevalent type of cancer globally, with an increasing incidence [1, 2]. Majority of BCC cases manifest on the head or neck and it could also affect the trunk and extremities. Although its mortality rate is relatively low, it still has a significant impact on patients' health and quality of life due to its destructive impact on the local tissues since the local tissue damage caused by BCC might cause significant morbidity and functional loss [3]. For instance, nasal and ocular periorbital tumors have the potential to result in vision loss [4]. At present, the treatment approaches for BCC mainly include surgical resection, radiotherapy and drug treatment [5]. However, due to the limited understanding of the pathogenesis of BCC, these treatments might not always be effective. The recurrence and resistance to treatment observed in some patients emphasize an urgent need for a deeper molecular understanding of BCC to provide information for the development of novel and targeted therapies [6, 7].

The cross-tissue association study has been widely applied to discover the candidate susceptibility genes for diseases recently [8–11]. Therefore, this study aims to identify susceptible genes and potential drug targets related to BCC by a cross-tissue transcriptome association study. Firstly, we performed a cross-tissue transcriptome association study to identify the candidate genes of BCC. Secondly, the results of candidate genes in a single tissue were verified by functional summary-based imputation (FUSION) method, and candidate genes were further screened based on multi-marker Analysis of GenoMic Annotation (MAGMA) analysis. In addition, summary data-based Mendelian randomization (SMR) and colocalization analyses were further conducted to infer the causal relationship between candidate genes and BCC. GeneMANIA analysis was used to understand the functional significance of the identified candidate genes, and the druggability of the identified genes were evaluated in order to find and discover the potential candidate drugs for BCC. We hope to reveal the molecular mechanism of BCC and provide scientific basis for developing new prevention, diagnosis and treatment strategies for BCC.

2 Materials and methods

2.1 Study design

The study design is displayed in Fig. 1.

2.2 Data sources

FinnGen represents the most extensive medical research initiative in Finland, with its primary objective being to enhance our comprehension of the genetic background of various diseases. Data from the GWAS on BCC were derived from the FinnGen R11 dataset (https://www.finngen.fi/en), encompassing a total of 23,424 European ancestry cases and 345,118 European ancestry controls [12]. Another GWAS data of BCC from GWAS Catalog were used to replicated our discoveries (17,416 European ancestry cases, 375,455 European ancestry controls) [13]. The GTEx_V8 eQTL dataset (https://ftp.ebi.ac.uk/pub/databases/spot/eQTL/imported/GTEx_V8) includes a substantial collection of gene expression data obtained from a range of 49 distinct fresh frozen tissues.

2.3 Cross-tissue and single-tissue TWAS analyses

The unified test for molecular signatures (UTMOST) analysis was conducted across various tissues to furnish a comprehensive assessment of the overall associations between gene expression and traits at the organismal scale [14]. This approach facilitates the detection of a greater number of genes that exhibit heightened trait heritability across tissues, thereby enhancing the precision of the estimation. The FUSION analysis was executed utilizing GWAS data of BCC along with the GTEx_V8 eQTL data of 49 different tissues, aiming to evaluate the relationships between these genes and BCC

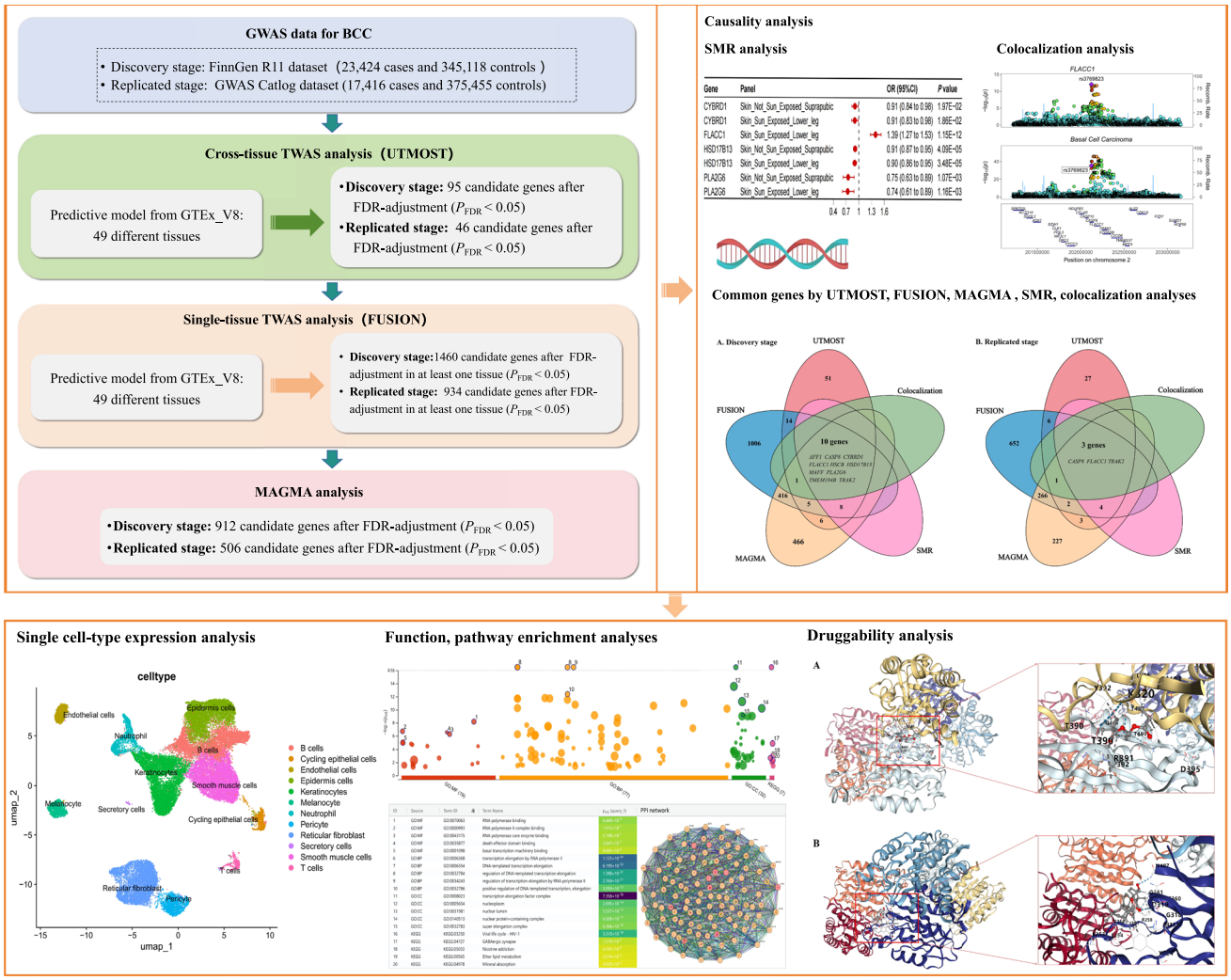

Fig. 1 Study design. *TWAS* transcriptome-wide association study, *UTMOST* unified test for molecular signatures, *GWAS* genome-wide association, *GTEx* Genotype-Tissues Expression Project, *FDR* false discovery rate, *FUSION* functional summary-based imputation, *MAGMA* multi-marker Analysis of GenoMic Annotation

[15]. The *P*-values were adjusted by the Benjamini–Hochberg approach to manage the false discovery rate (FDR), with a significance level set at α = 0.05. A *P*-value for FDR-adjustment (P_{FDR}) < 0.05 was considered to be statistically significant.

2.4 Conditional and joint analysis

The conditional and joint (COJO) analysis was conducted to identify the independent genetic signals, as the FUSION analysis could potentially reveal several correlated characteristics within a single genomic location [16]. Upon completion of the testing, genes that exhibited independent associations were designated as jointly significant, whereas those that no longer demonstrated significance were classified as marginally significant.

2.5 MAGMA analysis

We conducted the MAGMA analysis to amalgamate the association statistics of SNP level into the gene score, a process which quantifies the extent of association between each gene and the phenotype [17]. After applying the FDR adjustment, P_{FDR} < 0.05 was deemed to indicate statistical significance.

2.6 SMR analysis

Summary data-based Mendelian randomization (SMR) and colocalization analyses were performed to further investigate the causal relationships of identified genes with BCC. The top associated cis-expression quantitative trait loci (cis-eQTL) was selected by focusing on a window surrounding the corresponding gene (± 1000 kb) and applying a stringent *P*-value threshold of 5.0×10^{-8} [18]. The impact of SMR was assessed using the Wald ratio method, with a threshold for significance set at $P < 0.05$. The heterogeneity in the dependent instrument (HEIDI) test was utilized to differentiate between pleiotropic effects and those due to linkage, where the $P_{HEIDI} < 0.01$ were excluded from the analysis, as these were suspected to be potentially influenced by pleiotropy.

2.7 Colocalization analysis

In the colocalization analysis, a posterior probability of H4 (PP.H4) exceeding 0.70 was deemed supportive of colocalization, indicating a shared causal variant between the eQTL and GWAS. Specifically, a PP.H4 value above 0.90 was considered to provide strong evidence for colocalization.

2.8 Single cell-type expression analysis in BCC tissues

We used the single-cell RNA sequencing data from 4 BCC samples from the Gene Expression Omnibus (GEO) database (Registration number: GSE141526). The Seurat R package (v.5.1.0) was employed to analyze the data. To achieve high-quality single-cell RNA expression data, the following filtering criteria were established: 1. exclusion of cells that have a measured gene count below 300 or exceeding 7000; 2. exclusion of cells where mitochondrial contamination exceeds 10%. In total, 37,004 high-quality cells were retained for subsequent analysis. Post-quality control data would be normalized utilizing the "NormalizeData" function. The cell type annotation and clustering analysis were also performed by the Seurat R package (v.5.1.0).

2.9 Function and pathway enrichment analysis

The GeneMANIA platform (https://genemania.org/) was employed to elucidate the biological roles of each identified gene. STRING database (https://cn.string-db.org/) was used to predict the top 50 proteins interacting with these identified targets and construct the Protein–Protein Interaction (PPI) network. Gene Ontology (GO) and Kyoto Encyclopedia of Genes and Genomes (KEGG) analyses were performed by g: Profiler (https://biit.cs.ut.ee/gprofiler).

2.10 Disease connection of identified genes in mouse

For these identified genes, we employed the Mouse Genome Informatics (MGI) website (http://www.informatics.jax.org) to investigate their biological function and disease connection in the mouse models.

2.11 Druggability of the identified genes

The drug databases of DrugBank (https://go.drugbank.com/), and Therapeutic Target Database (https://db.idrblab.net/ttd/) were searched to evaluate the druggability of candidate genes of BCC. Molecular docking was conducted to evaluate the affinity of candidate drugs on their targeted proteins.

3 Results

3.1 Cross-tissue and single-tissue TWAS results

There were 448 genes were significantly associated with BCC (*P* value < 0.05) in cross-tissue TWAS analysis. Among them, 95 genes were still significant after the FDR adjustment (Table S1). In the replicated stage, 46 significant

genes were identified (Table S2). For the single-tissue TWAS analysis, a total of 1460 genes were identified with a P_{FDR} value < 0.05 for at least one tissue (Table S3), while 934 significantly genes were found in the replicated stage (Table S4). Thirty-eight significant genes were identified by both cross-tissue and single-tissue TWAS analyses. These candidate genes were *AFF1, ANKRD36BP2, ANTXR1, ATL2, C22orf31, C2CD6, CASP10, CASP8, CDK15, CFLAR-AS1, CLK1, CYBRD1, FLACC1, FZD7, HSCB, HSD17B11, HSD17B13, HYCC2, IGKC, IGKJ2, IGKV6-21, KCTD18, KIAA2012-AS1, KLHL8, MAFF, NDUFB3, NEMP2, PLA2G6, SCYL2P1, SLC16A8, STRADB, THOC1, THOC5, TMEM184B, TMEM237, TRAK2, UBE2CP2,* and *XBP1*.

3.2 COJO results

The 38 identified genes are primarily on chromosomes 2, 4, 18 and 22. The COJO analysis was conducted in related tissues to dispel false positive outcomes caused by LD. The TWAS signal of *CASP8* was significantly decreased under predicted *FLACC1* expression conditions in multiple tissues. The condition of predicted expression of *MAFF* and *PLA2G6* resulted in a significant reduction in TWAS signal of *TMEM184B* in multiple tissues. In Breast_Mammary_Tissue, under conditions of predicted *IGKJ2* expression, TWAS signals were significantly reduced in *IGKC* and *ANKRD36BP2* (Fig. 2). Since IGKC was only significant in the TWAS results for a single tissue and LD had a potential impact on this result, this gene was not considered in further analyses.

3.3 MAGMA results

A total of 912 significant genes were identified to be associated with the risk of BCC after the FDR adjustment in the MAGMA analysis (P_{FDR} < 0.05) (Table S5), and 506 significantly genes were found in the replicated stage (Table S6). After integrating with the findings of cross-tissue (UTMOST) and single-tissue (FUSION) TWAS analyses, there were still 24 genes significantly associated with BCC. These genes were *AFF1, ANTXR1, C2CD6, CASP10, CASP8, CDK15, CLK1, CYBRD1, FLACC1, FZD7, HSCB, HSD17B13, HYCC2, KCTD18, KLHL8, MAFF, NDUFB3, PLA2G6, STRADB, THOC5, TMEM184B, TMEM237, TRAK2,* and *XBP1*.

3.4 SMR results

The results of SMR analysis were presented in Table S7. The SMR analysis indicated that there were causal associations between 18 identified genes (*AFF1, C2CD6, CASP10, CASP8, CDK15, CYBRD1, FLACC1, FZD7, HSCB, HSD17B13, KLHL8, MAFF, PLA2G6, STRADB, TMEM184B, TMEM237, TRAK2,* and *XBP1*) and BCC (*P* value < 0.05). *C2CD6, CASP10, CASP8, FLACC1, STRADB, TMEM237,* and *TRAK2* genes were confirmed in the replicated stage (Table S8). Among them, *CASP8, CYBRD1, FLACC1, FZD7, HSD17B13, PLA2G6, STRADB,* and *TMEM184B* were associated with BCC in multiple tissues. In addition, *CYBRD1, FLACC1, HSD17B13* and *PLA2G6* were associated with BCC in Skin_Not_Sun_Exposed_Suprapubic and

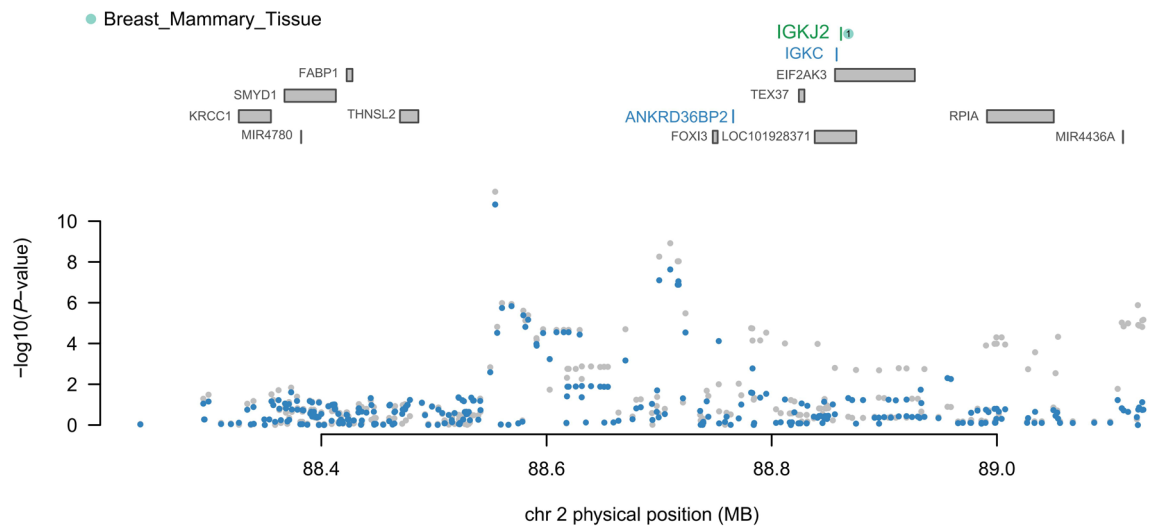

Fig. 2 COJO analysis results of IGKC. The jointly significant genes were shown in green and the marginally associated genes were displayed in blue

Skin_Sun_Exposed_Lower_leg tissues (Fig. 3). Among them, the association between *FLACC1* and BCC in Skin_Not_Sun_Exposed_Suprapubic and Skin_Sun_Exposed_Lower_leg tissues was replicated by using another GWAS data.

3.5 Colocalization results

The colocalization analysis suggested that there was evidence of colocalization supported by the *AFF1, ANTXR1, CASP8, CYBRD1, FLACC1, HSCB, HSD17B13, MAFF, PLA2G6, TMEM184B, TRAK2* genes and BCC (PP.H4 > 0.70; Table S9). The evidence of colocalization supported by the *CASP8, FLACC1, TRAK2* genes and BCC were confirmed in the replicated stage (PP.H4 > 0.70; Table S10). In addition, *CASP8, FLACC1, HSD17B13, MAFF,* and *PLA2G6* genes were supported by high colocalization evidence with BCC in several tissues (PP.H4 > 0.90). In particular, *FLACC1* and *TMEM184B* genes were supported by colocalization evidence with BCC in Skin_Not_Sun_Exposed_Suprapubic tissue, where the colocalization evidence between *FLACC1* and BCC was validated in the replicated stage (Fig. 4).

Ten genes (*AFF1, CASP8, CYBRD1, FLACC1, HSCB, HSD17B13, MAFF, PLA2G6, TMEM184B, TRAK2*) were both identified by UTMOST, FUSION, MAGMA, SMR and colocalization analyses in the discovery stage (Fig. 5A), while 3 genes (*CASP8, FLACC1, TRAK2*) were validated in the replicated stage (Fig. 5B).

3.6 Results of single-cell analysis in BCC tissues

As shown in Fig. 6, after cell types annotation, all cells were divided into 12 clusters incorporating B cells, cycling epithelial cells, endothelial cells, epidermis cells, keratinocytes, melanocyte, neutrophil, pericyte, reticular fibroblast, secretory cells, smooth muscle cells and T cells. The cell type gene expressions of identified genes were shown in Fig. 6B and C. Among these identified genes, *MAFF* was enriched in endothelial cells, reticular fibroblast, pericyte, and B cells.

3.7 Results of GeneMANIA analysis, PPI and enrichment analyses

The potential interacting gene networks constructed with these identified genes as the core were presented in Fig. 7. Among these identified genes, *CASP8*-related gene network had the largest number of signaling pathways, of which the most important functional pathways are the regulation of extrinsic apoptotic signaling pathway via death domain receptors, extrinsic apoptotic signaling pathway via death domain receptors, and regulation of cysteine-type endopeptidase activity involved in apoptotic process. The information for important functional pathways of other gene networks were displayed in Table S11.

A total of 100 proteins were identified interacting with these 10 targets. The results of PPI network, GO and KEGG analyses were displayed in Fig. 8. The mainly molecular function (MF) items were RNA polymerase binding, RNA polymerase II complex binding, death effector domain binding, RNA polymerase core enzyme binding, and basal transcription machinery binding. The major biological process (BP) were transcription elongation by RNA polymerase II, DNA-templated transcription elongation, regulation of DNA-templated transcription elongation, regulation of transcription elongation by RNA polymerase IIG, and positive regulation of DNA-templated transcription, elongation. The primary cellular component (CC) items were transcription elongation factor complex, nucleoplasm, nuclear lumen, nuclear protein-containing complex and super elongation complex. KEGG analysis suggested that the mainly pathways were viral life cycle-HIV-1, GABAergic synapse, nicotine addiction, ether lipid metabolism, and mineral absorption.

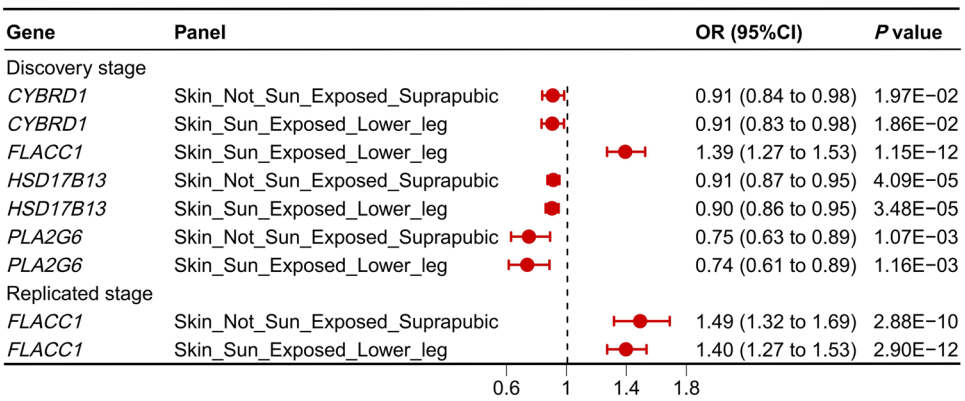

Fig. 3 SMR results of causal associations between identified genes and BCC in skin tissue

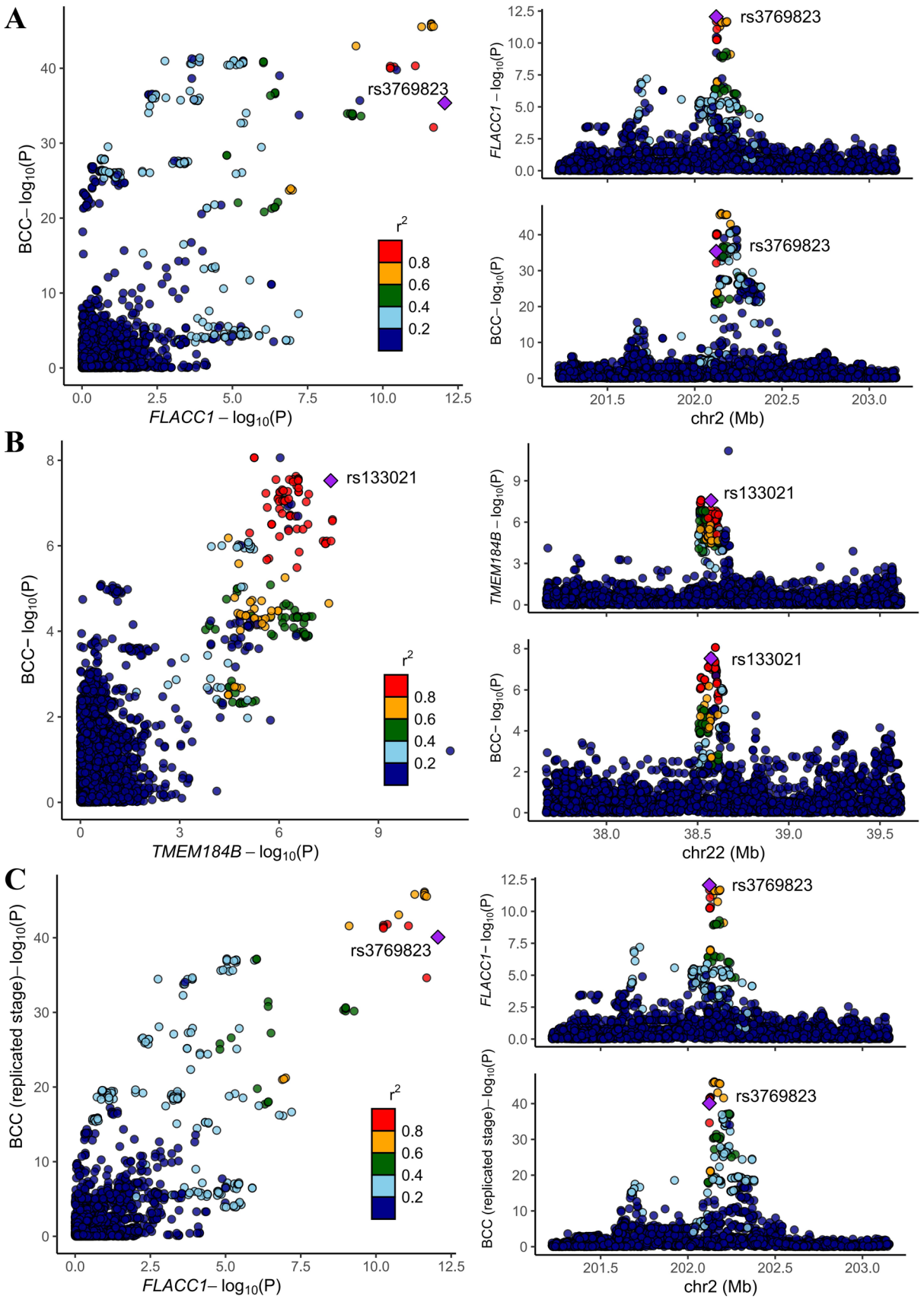

Fig. 4 The results of colocalization analysis between *FLACC1*, *TMEM184B* genes and BCC in Skin_Not_Sun_Exposed_Suprapubic tissue. **A** *FLACC1* in the discovery stage; **B** *TMEM184B* in the discovery stage; **C** *FLACC1* in the replicated stage

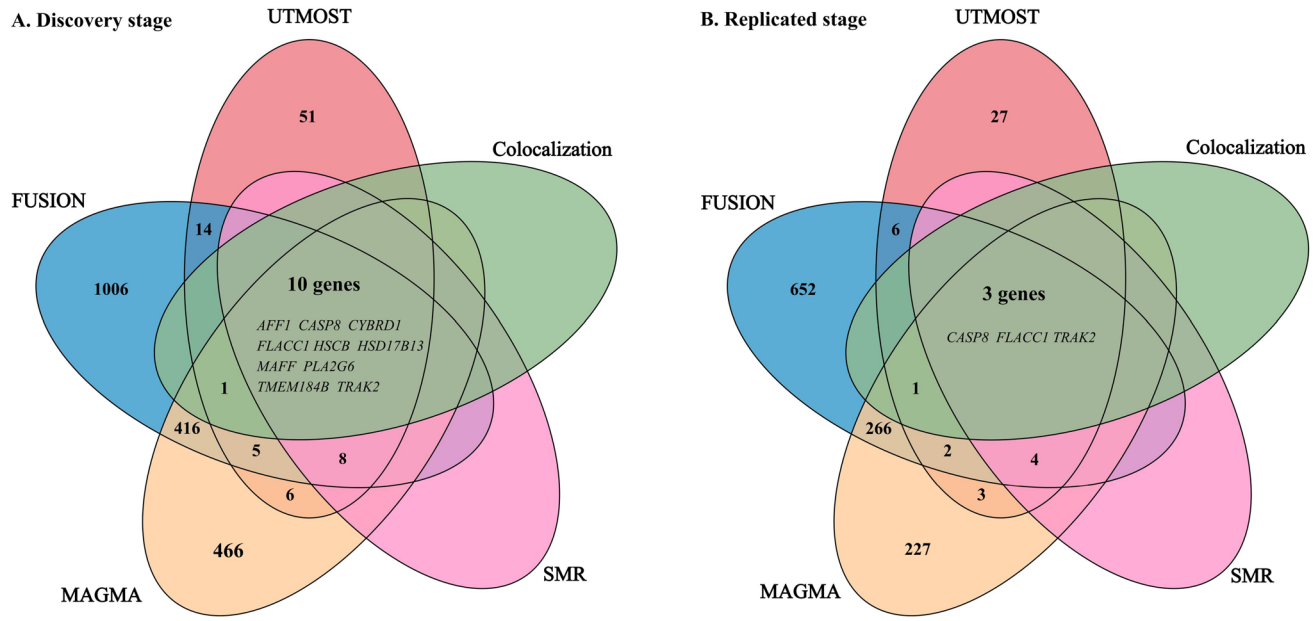

Fig. 5 Venn diagram. UTMOST, FUSION, MAGMA, SMR and colocalization analyses identified 10 common significant genes (discovery stage) and 3 common significant genes (replicated stage) associated with BCC risk

3.8 Disease connection analysis

The results of disease connection analysis were shown in Table S12. For the 10 identified target genes, *AFF1, CASP8, CYBRD1, FLACC1, HSD17B13, PLA2G6, TMEM184B* and *TRAK2* were reported to be associated with abnormal mouse phenotypes in multiple systems including cellular, integument, thomeostasis/metabolism, immune system, and muscle systems.

3.9 Druggability of identified genes

The druggability information for these identified genes was listed in Table S13. There were 6 investigational drugs targeting for *CASP8*. Among them, AN-9 was investigated for use/treatment in liver cancer, lung cancer, melanoma, and leukemia (lymphoid). Amooranin was also investigated for treatment in solid tumour/cancer. Two drugs targeting for *CYBRD1* were approved mainly for the prevention and treatment of iron deficiency anemia. GSK4532990 was designed to target *HSD17B13* for the treatment of non-alcoholic steatohepatitis. There was no information about *AFF1, FLACC1, HSCB, MAFF, PLA2G6, TMEM184B,* and *TRAK2*.

Among these investigational or approved drugs, AN-9 and amooranin seemed to have effects on BCC. We further performed molecular docking to evaluate the affinity of these drugs on their targeted proteins. The result was shown in Fig. 9. The lowest binding energies for interactions between AN-9 and CASP8 protein, and between amoracin and CASP8 protein were − 6.0 kcal/mol and − 7.2 kcal/mol, respectively, indicated stable bindings, which highlighted their potential as drug candidates.

4 Discussion

In the present study, we have systematically evaluated the association between gene expression and BCC risk though multiple methods including cross-tissue TWAS, single-tissue TWAS, MAGMA, SMR and colocalization analyses. A total of 10 candidate genes (*AFF1, CASP8, CYBRD1, FLACC1, HSCB, HSD17B13, MAFF, PLA2G6, TMEM184B, TRAK2*) were revealed to be significantly associated with BCC risk. Among them, *CASP8, FLACC1,* and *TRAK2* were confirmed in the replicated stage. GeneMANIA analysis indicated that the potential interacting gene networks constructed with these identified genes as the core were involved in multiple signaling pathways. KEGG analysis indicated that these identified genes were mainly involved in viral life cycle-HIV-1, GABAergic synapse, nicotine addiction, ether lipid

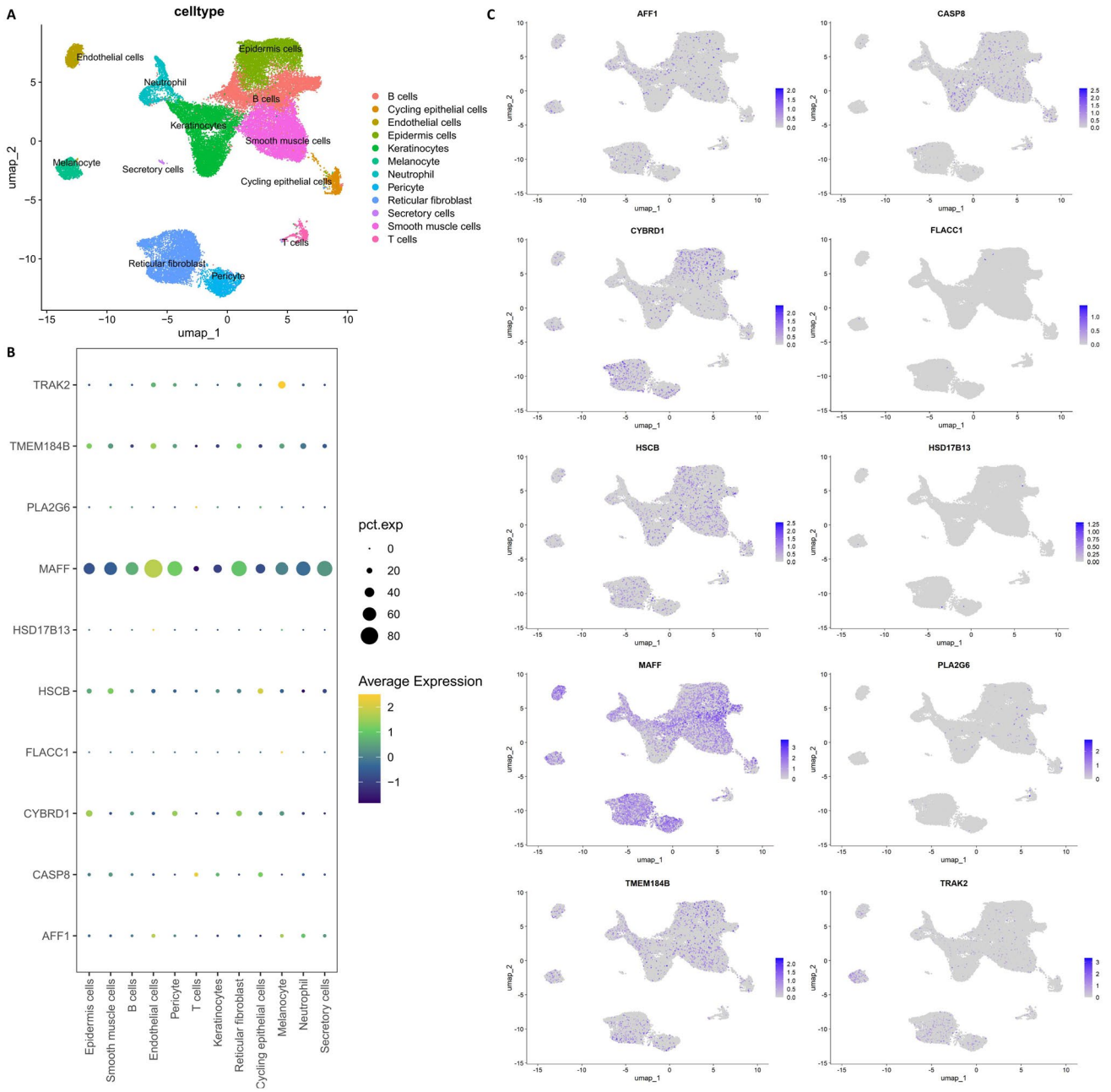

Fig. 6 Single-cell type expression in BCC tissue. **A** The 12 cell clusters labeled and annotated using marker genes; **B** and **C** The expression of identified genes in each cell type

metabolism, and mineral absorption pathways. Druggability analysis indicated that there were only 3 targets (*CASP8, CYBRD1 and HSD17B13*) with investigational or approved drugs. Among these drugs, AN-9 and amooranin might be candidate drugs for BCC since they marked stable bindings with *CASP8* protein.

CASP8 (caspase 8) is a gene encoding a member of the cysteine-aspartic acid protease (caspase) family, which acts as a pivotal regulatory enzyme for several forms of programmed cell death, including apoptosis, necroptosis, and pyroptosis [19]. *CASP8* was reported to be associated with various types of cancer such as ovarian cancer, breast cancer and renal cell carcinoma [20–22]. *FLACC1* (flagellum associated containing coiled-coil domains 1) was reported to be predisposing factors for development of cardiac autonomic neuropathy [23]. The mitochondrial adaptor *TRAK2* (trafficking kinesin protein 2) serves as a crucial activator that establishes a functional connection between the

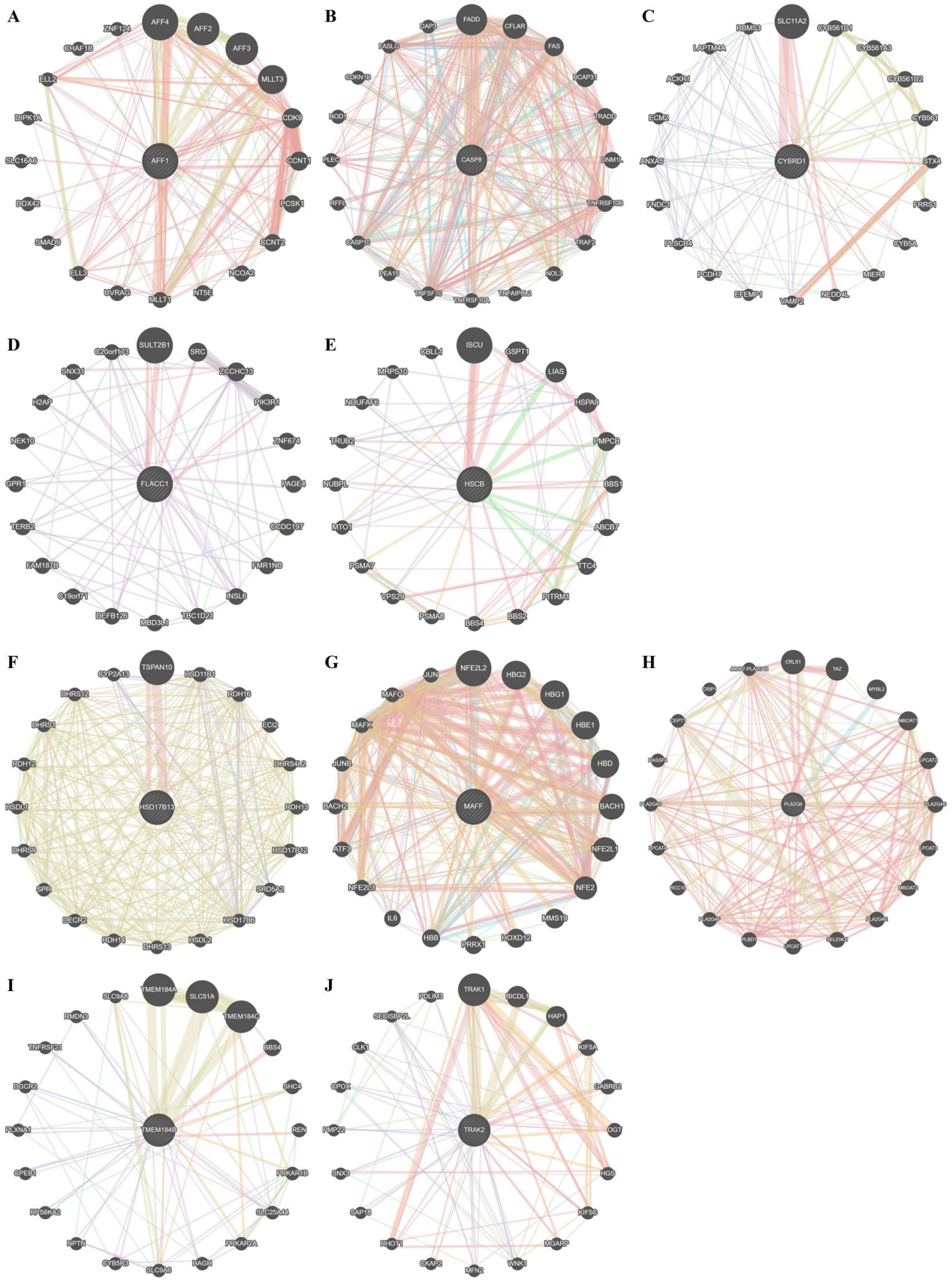

Fig. 7 GeneMANIA gene network. **A** *AFF1* as the core; **B** *CASP8* as the core; **C** *CYBRD1* as the core; **D** *FLACC1* as the core; **E** *HSCB* as the core; **F** *HSD17B13* as the core; **G** *MAFF* as the core; **H** *PLA2G6* as the core; **I** *TMEM184B* as the core; **J** *TRAK2* as the core

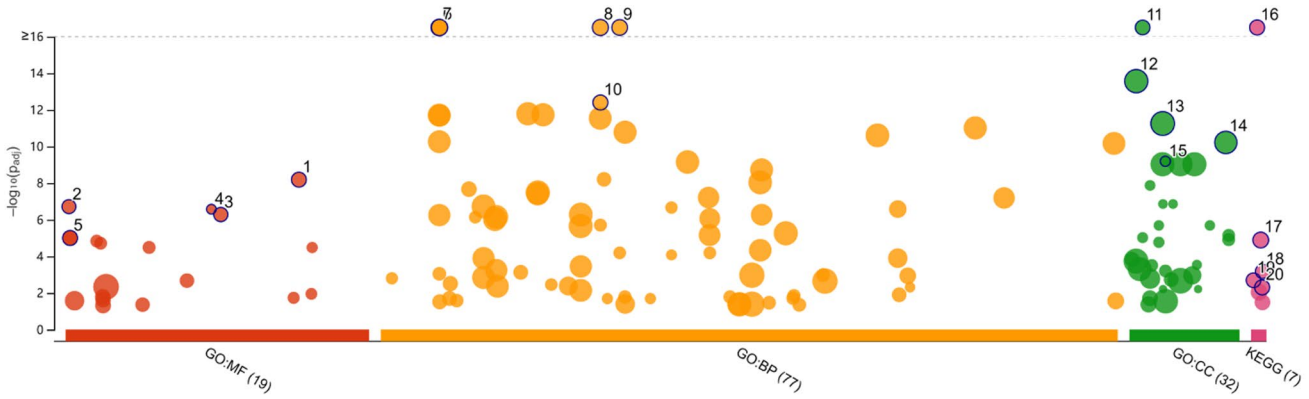

ID	Source	Term ID	Term Name	p_{adj} (query_1)
1	GO:MF	GO:0070063	RNA polymerase binding	6.449×10^{-9}
2	GO:MF	GO:0000993	RNA polymerase II complex binding	1.915×10^{-7}
3	GO:MF	GO:0043175	RNA polymerase core enzyme binding	5.198×10^{-7}
4	GO:MF	GO:0035877	death effector domain binding	2.647×10^{-7}
5	GO:MF	GO:0001098	basal transcription machinery binding	9.891×10^{-6}
6	GO:BP	GO:0006368	transcription elongation by RNA polymerase II	1.125×10^{-34}
7	GO:BP	GO:0006354	DNA-templated transcription elongation	6.199×10^{-33}
8	GO:BP	GO:0032784	regulation of DNA-templated transcription elongation	1.398×10^{-21}
9	GO:BP	GO:0034243	regulation of transcription elongation by RNA polymerase II	2.769×10^{-21}
10	GO:BP	GO:0032786	positive regulation of DNA-templated transcription, elongation	3.959×10^{-13}
11	GO:CC	GO:0008023	transcription elongation factor complex	7.358×10^{-78}
12	GO:CC	GO:0005654	nucleoplasm	2.695×10^{-14}
13	GO:CC	GO:0031981	nuclear lumen	5.537×10^{-12}
14	GO:CC	GO:0140513	nuclear protein-containing complex	6.008×10^{-11}
15	GO:CC	GO:0032783	super elongation complex	6.396×10^{-10}
16	KEGG	KEGG:03250	Viral life cycle - HIV-1	3.310×10^{-18}
17	KEGG	KEGG:04727	GABAergic synapse	1.279×10^{-5}
18	KEGG	KEGG:05033	Nicotine addiction	6.591×10^{-4}
19	KEGG	KEGG:00565	Ether lipid metabolism	2.014×10^{-3}
20	KEGG	KEGG:04978	Mineral absorption	4.929×10^{-3}

PPI network

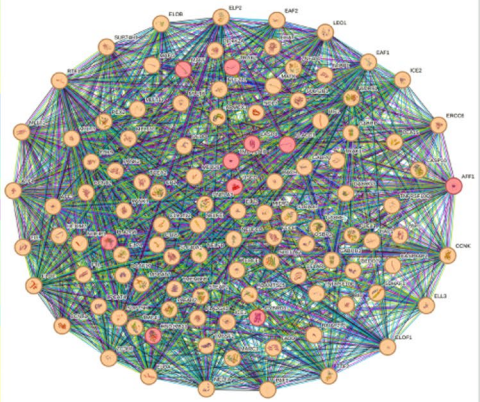

Fig. 8 PPI network, GO and KEGG analyses

opposing forces of kinesin and dynein motor proteins [24]. These 3 genes were discovered and validated to be significantly associated with the risk of BCC in our analyses and might be promising therapeutic targets for BCC.

AFF1 (ALF transcription elongation factor 1), recognized as a pivotal structural component of the super elongation complex (SEC), exerts control over the process of gene transcription. *AFF1* was reported to inhibit adipogenic differentiation through modulating *TGM2* transcription [25]. *CYBRD1* (cytochrome b reductase 1) belonging to the cytochrome b (561) family, is a gene that encodes for an iron-regulated protein. *CYBRD1* was also reported to be related with several types of cancer including hepatocellular carcinoma, ovarian cancer, colorectal cancer, etc. [26–28]. *HSCB* (HscB mitochondrial iron-sulfur cluster cochaperone) gene is responsible for encoding a DnaJ-like co-chaperone protein, which is a constituent of the heat shock cognate B (HscB) protein family. The encoded protein could potentially enhance the ATPase activity of the mitochondrial stress-70 protein. A loss-of-function variant in *HSD17B13* (hydroxysteroid 17-beta dehydrogenase 13) was correlated with a decreased likelihood of developing chronic liver disease and a slowed progression from fatty liver (steatosis) to a more severe inflammation condition (steatohepatitis) [29]. *MAFF* (MAF bZIP transcription factor F) gene encodes for a basic leucine zipper (bZIP) transcription factor, characterized by the absence of a transactivation domain. *MAFF* plays a role in increasing the susceptibility of lung adenocarcinoma to cisplatin-based chemotherapy and ionizing radiation by influencing the processes of ferroptosis and the advancement of the cell cycle [30]. The protein encoded by *PLA2G6* (phospholipase A2 group VI) is an A2 phospholipase enzyme, which facilitates the detachment of fatty acids from phospholipids. *PLA2G6* was mainly associated with neurodegenerative diseases [31]. *TMEM184B* (transmembrane protein 184B) plays a pivotal role in fostering the proliferation, migration, and invasiveness of hypopharyngeal squamous cell carcinoma cells, concurrently acting to suppress the process of apoptosis [32]. These 7 genes were discovered to be significantly associated with the risk of BCC in our analyses. Although they were not confirmed in the replicated stage, the GWAS data used in the discovery stage had a larger sample size, and hence the findings from the discovery stage were more credible.

The advantage of the present study is that multiple methods (UTMOST, FUSION, MAGMA, SMR and colocalization analyses) were employed to discover and validate BCC susceptibility genes, which contributed to the credibility and stability

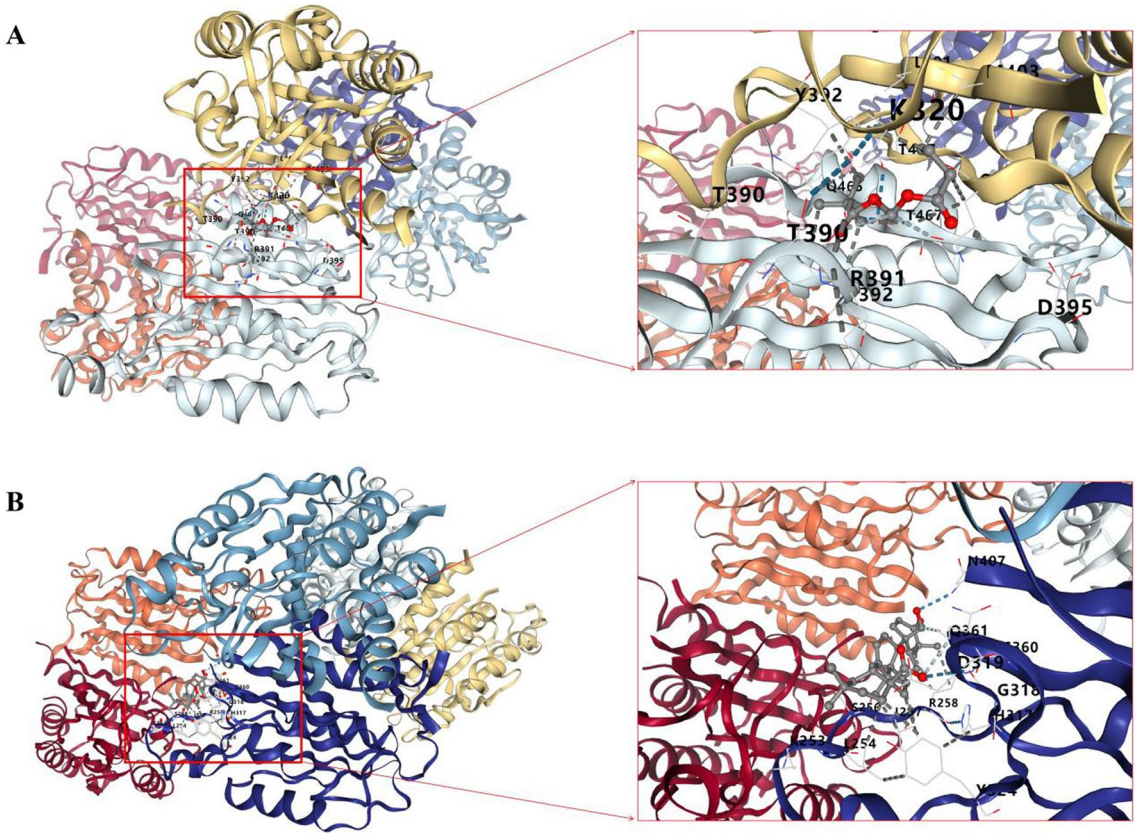

Fig. 9 Molecular docking analysis of CASP8 with AN-9 and amooranin. **A** AN-9; **B** Amooranin

of our results. There are also several limitations in this study. On the one hand, this study was conducted on a European population and there is a requirement for additional confirmation whether the identified targets are applicable to other populations. On the other hand, although the cross-tissue gene expression method is novel, the strategy used relies on the imputation of expression results and it probably could not capture the expression weights of all BCC-related genes. In addition, detailed clinical information on BCC cases is not available in the GWAS data, and it is not known whether other diseases (e.g., Gorlin syndrome) are included in the population. Furthermore, due to the lack of data, we are unable to perform subgroup analyses based on sex, age at diagnosis, and major BCC subtypes (infiltrative, superficial, or nodular), nor can we conduct polygenic risk score (PRS) analysis based on the lead independent genome-wide significant SNPs for BCC count, to explore whether this trait is associated with differences in BCC across sex, age, and phenotypic subtypes. Future studies that focus on factors like sex, age, phenotypic subtypes and BCC count are essential to uncover genetic variants associated with these specific subgroups.

5 Conclusion

In conclusion, these findings not only help us better understand the molecular pathology of BCC, but also provide potential molecular markers and therapeutic targets for future personalized medicine. Through further research on the function and mechanism of these genes, we hope to develop more effective and targeted treatment methods to improve the prognosis and quality of life in BCC patients. This study is expected to provide a new perspective for BCC's precision medicine and lay a foundation for future clinical research and drug development.

Acknowledgements We appreciate the publicly available GWAS datasets for BCC as well as gene expression and eQTL data.

Author contributions HS has made contributions to the design of the work, the acquisition, analysis and interpretation of data, the drafting and revising of the article. LL and XX have made contributions to the acquisition and analysis of data. JY has made contributions to the design,

the administration of the project and revising of the article. TH has made contributions to the design of the work, the administration of the project, revising of the article and the acquisition of funding. All authors contributed to the article and approved the submitted version.

Funding This study was supported by grants from the Shanghai Municipal Health Commission (No. 202140069), and Science and Technology Commission of Shanghai Municipality (No. 23ZR1409100).

Data availability The data of FinnGen can be accessed at https://www.finngen.fi/en. The data of GWAS Catalog can be accessed at https://www.ebi.ac.uk/gwas. The GTEx_V8 eQTL dataset can be accessed at https://ftp.ebi.ac.uk/pub/databases/spot/eQTL/imported/GTEx_V8. The single-cell RNA sequencing data of BCC tissue can be accessed at https://www.ncbi.nlm.nih.gov/geo/query/acc.cgi?acc=GSE141526.

Declarations

Ethics approval and consent to participate Ethical approval was waived because this study used the data from publicly available databases.

Consent for publications Not applicable.

Competing interests The authors declare no competing interests.

References

1. Heath M, Bar A. Basal cell carcinoma. Dermatol Clin. 2023;41(1):13–21.
2. Dika E, Scarfì F, Ferracin M, Broseghini E, Marcelli E, Bortolani B, et al. Basal cell carcinoma: a comprehensive review. Int J Mol Sci. 2020;21(15):5572.
3. Kim D, Kus K, Ruiz E. Basal cell carcinoma review. Hematol Oncol Clin North Am. 2019;33(1):13–24.
4. Bengoa-González A, Mencía-Gutiérrez E, Garrido M, Salvador E, Lago-Llinás M. Advanced periocular basal cell carcinoma with orbital invasion: update on management and treatment advances. J Ophthalmol. 2024;2024:4347707.
5. Peris K, Fargnoli M, Kaufmann R, Arenberger P, Bastholt L, Seguin N, et al. European consensus-based interdisciplinary guideline for diagnosis and treatment of basal cell carcinoma—update 2023. Eur J Cancer. 2023;192:113254.
6. Habashy S, Jafri A, Osman HO, Thomas NE, Udekwe S, Heindl SE. Hedgehog pathway inhibitors: clinical implications and resistance in the treatment of basal cell carcinoma. Curēus. 2021;13(3):e13859.
7. Sooksamran A, Pichai P, Suphannaphong M, Singthong S. Previous therapy and the recurrence rate of basal cell carcinoma after Mohs surgery: a meta-analysis. Arch Dermatol Res. 2023;315(6):1747–54.
8. Gamazon E, Wheeler H, Shah K, Mozaffari S, Aquino-Michaels K, Carroll R, et al. A gene-based association method for mapping traits using reference transcriptome data. Nat Genet. 2015;47(9):1091–8.
9. Sekita A, Kawasaki H, Fukushima-Nomura A, Yashiro K, Tanese K, Toshima S, et al. Multifaceted analysis of cross-tissue tran- scriptomes reveals phenotype—endotype associations in atopic dermatitis. Nat Commun. 2023;14(1):6133.
10. Silva T, Young J, Zhang L, Gomez L, Schmidt M, Varma A, et al. Cross-tissue analysis ofblood and brain epigenome-wide association studies in Alzheimer'sdisease. Nat Commun. 2022;13(1):4852.
11. Tang H, Wang J, Deng P, Li Y, Cao Y, Yi B, et al. Transcriptome-wide association study-derived genes as potential visceral adipose tissue-specific targets for type 2 diabetes. Diabetologia. 2023;66(11):2087–100.
12. Kurki MI, Karjalainen J, Palta P, Sipila TP, Kristiansson K, Donner KM, et al. FinnGen provides genetic insights from a well-phenotyped isolated population. Nature. 2023;613(7944):508–18.
13. Adolphe C, Xue A, Fard AT, Genovesi LA, Yang J, Wainwright BJ. Genetic and functional interaction network analysis reveals global enrichment of regulatory T cell genes influencing basal cell carcinoma susceptibility. Genome Med. 2021;13(1):19.
14. Hu Y, Li M, Lu Q, Weng H, Wang J, Zekavat S, et al. A statistical framework for cross-tissue transcriptome-wide association analysis. Nat Genet. 2019;51(3):568–76.
15. Gusev A, Ko A, Shi H, Bhatia G, Chung W, Penninx BWJH, et al. Integrative approaches for large-scale transcriptome-wide association studies. Nat Genet. 2016;48(3):245–52.
16. Deng Y, Pan W. Improved use of small reference panels for conditional and joint analysis with GWAS summary statistics. Genetics. 2018;209(2):401–8.
17. de Leeuw CA, Mooij JM, Heskes T, Posthuma D. MAGMA: generalized gene-set analysis of GWAS data. Plos Comput Biol. 2015;11(4):e1004219.
18. Sun H, Li L, Yan J, Huang T. Prioritization of drug targets for thyroid cancer: a multi-omics Mendelian randomization study. Endocrine. 2024;86(2):732–43. https://doi.org/10.1007/s12020-024-03933-x.

19. Fritsch M, Günther S, Schwarzer R, Albert M, Schorn F, Werthenbach J, et al. Caspase-8 is the molecular switch for apoptosis, necroptosis and pyroptosis. Nature. 2019;575(7784):683–7.
20. Ma X, Zhang J, Liu S, Huang Y, Chen B, Wang D. Polymorphisms in the CASP8 gene and the risk of epithelial ovarian cancer. Gynecol Oncol. 2011;122(3):554–9.
21. Vahednia E, Shandiz F, Bagherabad M, Moezzi A, Afzaljavan F, Tajbakhsh A, et al. The impact of CASP8 rs10931936 and rs1045485 polymorphisms as well as the haplotypes on breast cancer risk: a case-control study. Clin Breast Cancer. 2019;19(5):e563–77.
22. Li T, Liu N, Zhang G, Chen M. CASP4 and CASP8 as newly defined autophagy-pyroptosis-related genes associated with clinical and prognostic features of renal cell carcinoma. J Cancer Res Ther. 2022;18(7):1952–60.
23. Bekenova N, Sibagatova A, Aitkaliyev A, Vochshenkova T, Kassiyeva B, Benberin V. Genetic markers of cardiac autonomic neuropathy in the Kazakh population. Bmc Cardiovasc Disord. 2024;24(1):242.
24. Fenton AR, Jongens TA, Holzbaur E. Mitochondrial adaptor TRAK2 activates and functionally links opposing kinesin and dynein motors. Nat Commun. 2021;12(1):4578.
25. Chen Y, Wang Y, Lin W, Sheng R, Wu Y, Xu R, et al. AFF1 inhibits adipogenic differentiation via targeting TGM2 transcription. Cell Prolif. 2020;53(6):e12831.
26. Wroblewska A, Woziwodzka A, Rybicka M, Bielawski KP, Sikorska K. Polymorphisms related to iron homeostasis associate with liver disease in chronic hepatitis C. Viruses. 2023;15(8):1710.
27. Chen R, Cao J, Jiang W, Wang S, Cheng J. Upregulated expression of CYBRD1 predicts poor prognosis of patients with ovarian cancer. J Oncol. 2021;2021:7548406.
28. Zhao G, Wang Q, Zhang Y, Gu R, Liu M, Li Q, et al. DDX17 induces epithelial-mesenchymal transition and metastasis through the miR-149-3p/CYBRD1 pathway in colorectal cancer. Cell Death Dis. 2023;14(1):1.
29. Abul-Husn N, Cheng X, Li A, Xin Y, Schurmann C, Stevis P, et al. A protein-truncating HSD17B13 variant and protection from chronic liver disease. N Engl J Med. 2018;378(12):1096–106.
30. Liang J, Bi G, Huang Y, Zhao G, Sui Q, Zhang H, et al. MAFF confers vulnerability to cisplatin-based and ionizing radiation treatments by modulating ferroptosis and cell cycle progression in lung adenocarcinoma. Drug Resist Updat. 2024;73:101057.
31. Deng X, Yuan L, Jankovic J, Deng H. The role of the PLA2G6 gene in neurodegenerative diseases. Ageing Res Rev. 2023;89:101957.
32. Lin Y, Liu D, Li X, Ma Y, Pan X. TMEM184B promotes proliferation, migration and invasion, and inhibits apoptosis in hypopharyngeal squamous cell carcinoma. J Cell Mol Med. 2022;26(21):5551–61.